JOURNAL OF CATALYSIS 105, 95–106 (1987)

# Surface Chemistry and Catalytic Activity of $La_{1-y}M_yCoO_3$ Perovskite (M = Sr or Th)

## 1. Bulk and Surface Reduction Studies

J. A. MARCOS,* R. H. BUITRAGO,† AND E. A. LOMBARDO*,[1]

*Instituto de Investigaciones en Catálisis y Petroquímica (INCAPE) and †Instituto de Desarrollo Tecnológico para la Industria Química (INTEC) Universidad Nacional del Litoral, Consejo Nacional de Investigaciones Científicas y Técnicas, 3000 Santa Fe, Argentina

Received November 1985; revised December 8, 1986

The extent of bulk reduction of the mixed oxides in hydrogen, at temperatures between 250 and 500°C, was measured using a gas recirculating batch reactor connected to a standard BET high-vacuum system ($10^{-3}$ Pa). The hydrogen treatment was also performed in a chamber attached to an ESCA spectrometer to obtain information about the surface modifications produced upon reduction. In these mixed oxides cobalt is the only cation that can be reduced to its metallic state within the temperature range explored. Both systems included a trap which was either cooled with liquid air or left at room temperature to study the effect of the water arising from the hydrogen treatment upon both the rate and the extent of reduction. The bulk measurements have shown that the presence of water impairs the reduction process. The XPS studies have also substantiated this effect at the surface level. In the absence of water the metallic cobalt is segregated to the surface at reduction temperatures above 300°C. When water is present, lower concentrations of $Co^0$ appear on the surface and the segregation of this element is impaired. When thorium partially replaces lanthanum that element is not affected by the hydrogen treatment at any temperature up to 500°C. In the $La_{0.6}Sr_{0.4}CoO_3$ system, the SrO begins to segregate, whether or not water is present, at temperatures higher than 250°C. This mixed oxide is in fact the easiest to reduce. After reduction, even with the trap cooled with liquid air, the XPS spectra show a sharp increase in hydroxyl concentration. This effect increases in the direction Th < La < Sr, as expected from the similar trend of their Pauling electronegativity values. At high extents of reduction it was found that these hydroxyl groups were able to reoxidize the surface $Co^0$ upon evacuation in the ESCA spectrometer. This effect is less pronounced in going from the Sr- to the Th-containing oxide, with the $LaCoO_3$ showing an intermediate behavior. The reduction model proposed for the lanthanum cobaltate by E. A. Lombardo, K. Tanaka, and I. Toyoshima (*J. Catal.* **80**, 1983) has been improved and extended to the other cobalt mixed oxides. © 1987 Academic Press, Inc.

### INTRODUCTION

The reduction of $LaCoO_3$ perovskite under controlled conditions produces a solid containing $Co^0$ dispersed in an oxide matrix which catalyzes the hydrogenation and hydrogenolysis of several simple hydrocarbons (*1–3*). Both the activity and the selectivity of the reactions studied are strongly affected by the temperature of pretreatment in hydrogen in such a manner that they cannot be linearly correlated with the extent of reduction of the bulk.

Sis *et al.* (*4*) have studied the volumetric reduction of the lanthanum cobaltate. Through the measurement of the magnetic moment of the solid along the reduction process, they have found that a ferromagnetic phase ($Co^0$) started to form at or below 300°C. They suggested the following reaction scheme:

$$LaCoO_3 + yH_2 \rightarrow LaCo_xO_{3-y} + (1-x)Co^0 + yH_2O \quad (<400°C) \quad (1)$$

$$2LaCo_xO_{3-y} + (3-2y)H_2 \rightarrow 2xCo^0 + La_2O_3 + (3-2y)H_2O \quad (>400°C). \quad (2)$$

Crespin and Hall (*5*) have also studied

[1] To whom all correspondence should be addressed.



0021-9517/87 $3.00
Copyright © 1987 by Academic Press, Inc.
All rights of reproduction in any form reserved.

the reduction of the same crystalline mixed oxide. They conducted the reduction in a recirculation system, measured the hydrogen uptake, and followed the structural changes through X-ray diffraction (XRD). Although they agree with Sis *et al.* (*4*) in suggesting a two-step mechanism, they have proposed a different reaction for the first step:

$$LaCoO_3 + 0.5H_2 \rightarrow LaCoO_{2.5} + 0.5\ H_2O \quad (400°C). \quad (3)$$

In their system, reaction (2) occurred at 500°C. They did not detect the XRD pattern of metallic cobalt even in the completely reduced sample ($Co^0/La_2O_3$). This indicates that very small $Co^0$ clusters, less than 30 Å in diameter, are formed upon reduction.

Lombardo *et al.* (*6*) have studied the surface reduction of $LaCoO_3$ by XPS. They have reported a sharp increase in $Co^0$ surface concentration at reduction temperatures around 350°C, followed by a partial reoxidation of the surface layer when the pretreatment with hydrogen was carried out at higher temperatures. The variation of $Co^0$ surface concentration with reduction temperature closely follows the changes in both catalytic activity for ethylene hydrogenation and carbon monoxide chemisorption at low temperature (−20°C). Although Lombardo *et al.* (*6*) speculated about possible causes of the reoxidation of cobalt at high temperatures, they could substantiate none of them.

It has been shown that the partial substitution of La in this and related mixed oxides modifies the metal–oxygen bond strength (*7*). In this way, it could be possible to modify their reduction behavior as well as their catalytic properties.

The present study was undertaken to further investigate the mechanism of reduction of $LaCoO_3$ and the effect of partial La substitution by either Th or Sr upon the reducibility of both the surface and the bulk of $La_{1-y}M_yCoO_3$ (M = Sr or Th).

## EXPERIMENTAL

*Mixed oxide preparation.* $LaCoO_3$ was prepared by precipitation of $La(NO_3)_3$ with $K_3[Co(CN)_6]$ (*6*). The lanthanum cobaltates partially substituted by either Sr or Th were prepared by freeze-drying. The appropriate nitrates were dissolved in water in adequate proportions to obtain a 0.5 *M* solution (total cation concentration). The solution was frozen by injection of droplets in liquid air and freeze-dried in a commercial unit. The dry solid was then fired in oxygen at 950°C for 16 h. More details about the technique have been given elsewhere (*8–10*).

The main characteristics of the oxides obtained are shown in Table 1. The XRD patterns of the $La_{0.8}Th_{0.2}CoO_3$ preparation showed distinct peaks of segregated $ThO_2$. This is not surprising since it is known that only small amounts of cations with higher oxidation states than the transition metal (Co) can be incorporated into the perovskite lattice (*7*). By comparison with a mechanical mixture of the perovskite and $ThO_2$ it was ascertained that between 50 and 75% of the Th was incorporated into the structure.

*Reduction procedures.* The bulk reduction data were obtained using a standard gas recirculating system (*1*) which included a liquid air trap. The extent of reduction was calculated from the hydrogen uptake. In a few experiments the trap was left at room temperature in order to ascertain the effect of the water formed during the reduction upon both the rate and extent of reduction.

To study the surface modifications that

TABLE 1

Physical Properties of the Mixed Oxides

| Mixed oxide | Calcination temperature (°C) | Surface area ($m^2/g$) | Structure |
|---|---|---|---|
| $LaCoO_3$ | 800 | 6 | Perovskite |
| $La_{0.6}Sr_{0.4}CoO_3$ | 950 | 4 | Perovskite |
| $La_{0.8}Th_{0.2}CoO_3$ | 950 | 2 | Perovskite + $ThO_2$ |

occur during reduction, a pretreatment chamber with a lateral cold trap, having a volume of 1 liter, was connected directly to an ESCA 750 Shimadzu instrument. This spectrometer is driven by a computer system (ESCAPAC 760) which allows both the accumulation of data and their processing.

The oxide powder was pelleted to form a tablet 6 mm in diameter, weighing approximately 10 mg. Each sample was subjected to the following treatment: (a) evacuation at 400°C, final pressure $<10^{-5}$ Pa, in the analyzer chamber, (b) reduction at the desired temperature, starting at 250–300°C, in the pretreatment chamber, (c) evacuation of the hydrogen after the probe has been cooled down at room temperature, (d) evacuation at 300°C in the analyzer chamber. The spectra were always taken at 300°C. This cycle was repeated at increasing reduction temperatures up to 500°C. At each temperature it was checked that the equilibrium extent of reduction was attained by repeating the hydrogen treatment and verifying that no additional cobalt reduction had occurred.

The effect of water was studied by repeating the same procedure with the trap either immersed in liquid air or left uncooled (room temperature). In the former case, the water pressure was essentially zero while in the latter it was calculated that a maximum water vapor pressure of about 100 Pa could be reached after complete reduction.

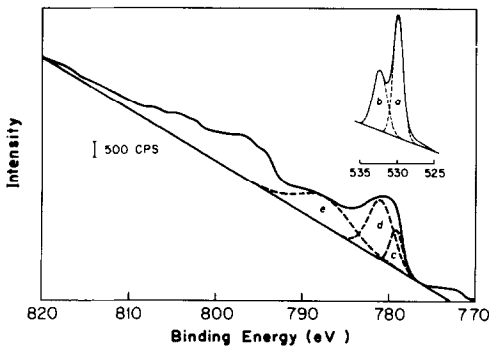


FIG. 1. Example of Co2$p_{3/2}$ and O1$s$ curve resolution. $LaCoO_3$ reduced at 300°C in dry $H_2$ ($p_{H_2} \simeq 1$ atm). (a) Lattice oxygen (BE 529.7 eV: FWHM 2.0 eV). (b) Surface OH (BE 532.2 eV; FWHM 2.8 eV). (c) $Co^0$ (BE 778.8 eV; FWHM 1.8 eV). (d) $Co^{2+}$ + $Co^{3+}$ (BE 780.4 eV; FWHM 4.1 eV). (e) Satellite peak (BE 786.7 eV; FWHM 6.6 eV).

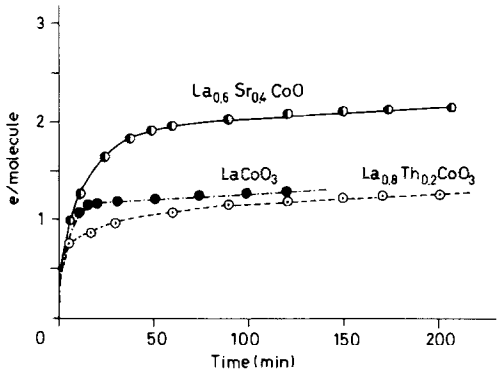


FIG. 2. Kinetic reduction curves of $La_{1-y}M_yCoO_3$ (M = Sr or Th) in $H_2$ at 350°C.

The hydrogen used in all the experiments was purified by passage through a Pd–Ag thimble.

*Treatment of data.* The atomic fraction of elements at the surface was calculated using the area under the peaks, the Scofield photoionization cross sections, the mean free paths of the electrons calculated as $\lambda \propto KE^{0.45}$, and the instrumental function given by the ESCA manufacturer (*11*), where KE means kinetic energy.

To estimate the contribution of $Co^0$, $Co^{2+}$, and $Co^{3+}$ to the Co2$p$ peaks the curve resolver Model CR-6B, included in the ESCAPAC unit, was used. This instrument permits one to work with Gaussian, Lorentzian, or mixed peaks up to a maximum of six. To resolve the O1$s$ peak into its components a similar procedure was used. An example of both the O1$s$ and the Co2$p$ signal resolution is shown in Fig. 1.

## RESULTS

### *Bulk Reduction*

$LaCoO_3$, $La_{0.8}Th_{0.2}CoO_3$, and $La_{0.6}Sr_{0.4}CoO_3$ were reduced in the gas recirculating system at temperatures between 250 and 500°C using a liquid air trap. The reduction curves obtained at each temperature

TABLE 2

Equilibrium Bulk Reduction of the Mixed Oxides[a]

| Reduction temperature (°C) | $LaCoO_3$ (*e*/molec) | $La_{0.8}Th_{0.2}CoO_2$ (*e*/molec) | $La_{0.6}Sr_{0.4}CoO_3$ (*e*/molec) |
|---|---|---|---|
| 250 | 0.4 | — | 0.7 |
| 300 | 1.2 | 1.1 | 1.3 |
| 350 | 1.3 | 1.4 | 2.2 |
| 400 | 1.4 | 1.6 | 2.4 |
| 450 | 2.4 | 2.9 | — |
| 500 | 3.0 | 2.9[b] | 3.3[b] |

[a] Reduction extent calculated from hydrogen uptake, measured in a gas recirculating system $p_{H_2}$ = 200 Torr. Complete reduction of $Co^{3+}$ to $Co^0$ corresponds to three electrons per formula weight of mixed oxide.

[b] The maximum reduction is lower or higher than 3 due to the presence of either $Co^2$ ($Th^{4+}$) or $Co^{4+}$ ($Sr^{2+}$).

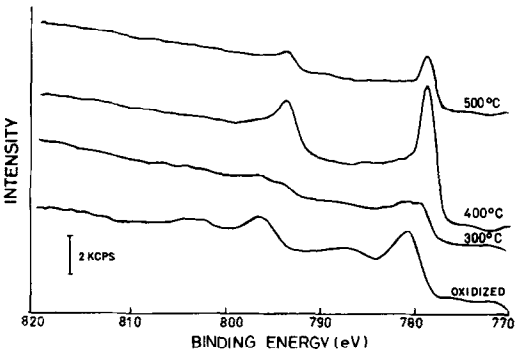


FIG. 3. Co2*p* spectra of $LaCoO_3$ before and after reduction at different temperatures. Liquid air cooled trap, $p_{H_2}$ = 1 atm.

were of the same shape as those shown in Fig. 2. The plateau values obtained at each temperature are collected in Table 2. Note that the cobalt is the only cation that can be reduced under these experimental conditions.

If the trap was not cooled, the reduction rate was significantly slower and no matter how high was the temperature (< 500°C) the reduction process stopped at intermediate values, i.e., ~1.5 electrons/molecule.

### *Surface Reduction*

*Experiments using the liquid air trap.* In the ESCA pretreatment chamber the reduction equilibrium was reached in 2 h. Tables 3 to 5 show the binding energy (BE) and the full width at half maximum (FWHM) of each element that make part of the three kind of oxides analyzed. In Fig. 3 the evolution of the Co2*p* spectra of $LaCoO_3$ as the reduction temperature increases up to 500°C is shown. Note that the peak width goes through a maximum at 300°C while the BE shifts to lower values at all reduction temperatures studied. This is also seen in Table 3. The changes that occur in the O1*s* signal as the reduction temperature increases up to 500°C are shown in Fig. 4. The O1*s* spectra is mainly a composite of two peaks. As shown in Fig 1, these peaks

TABLE 3

Binding Energies and FWHMs of $LaCoO_3$ Reduced in Dry $H_2$[a]

| Reduction temperature (°C) | Co2$p_{3/2}$ | | La3$d_{5/2}$ | | O1*s* | |
|---|---|---|---|---|---|---|
| | BE (eV) | FWHM (eV) | BE (eV) | FWHM (eV) | BE (eV) | FWHM (eV) |
| Oxide[b] | 780.6 | 4.3 | 834.7 | 6.9 | 529.7 | 1.8 |
| 300 | 779.2 | 5.4 | 835.1 | 6.8 | 530.1 | 1.8 |
| 350 | 779.1 | 2.7 | 835.2 | 6.8 | 530.1 | 2.0 |
| 400 | 779.1 | 2.3 | 835.2 | 6.7 | 530.1 | 4.1 |
| 450 | 779.1 | 2.2 | 835.2 | 6.7 | 530.1 | 4.2 |
| 480 | 779.1 | 2.2 | 835.3 | 6.7 | 532.3 | 3.9 |
| 500 | 779.1 | 2.2 | 835.5 | 6.6 | 532.2 | 3.8 |

[a] The reduction was carried out in the pretreatment chamber which has a liquid air cooled trap, $p_{H_2} \simeq 1$ atm.

[b] Evacuated at 400°C.

TABLE 4

Binding Energies and FWHMs of $La_{0.8}Th_{0.2}CoO_3$ Reduced in Dry $H_2$[a,b]

| Reduction temperature (°C) | Co2$p_{3/2}$ | | La3$d_{5/2}$ | | O1$s$ | |
|---|---|---|---|---|---|---|
| | BE (eV) | FWHM (eV) | BE (eV) | FWHM (eV) | BE (eV) | FWHM (eV) |
| Oxide | 780.7 | 4.6 | 834.9 | 7.2 | 529.8 | 2.1 |
| 300 | 779.2 | 5.2 | 835.2 | 6.9 | 529.9 | 2.2 |
| 350 | 779.0 | 2.2 | 835.4 | 6.8 | 530.2 | 2.2 |
| 400 | 778.9 | 2.2 | 835.5 | 6.8 | 530.3 | 2.0 |
| 450 | 778.8 | 2.0 | 835.5 | 6.7 | 530.2 | 2.0 |
| 500 | 778.8 | 2.0 | 835.6 | 6.8 | 530.2 | 2.0 |

[a] See footnotes in Table 3.

[b] The Th4$f_{7/2}$ BE and FWHM remained constant throughout the reduction process at 333.9 ± 0.1 and 2.0 ± 0.2 eV, respectively.

result from the addition of one located at lower BE (529.7 ± 0.2 eV), due to the lattice oxygen, and another at higher BE (532.2 ± 0.2 eV) assigned to hydroxyls, in agreement with Fleisch *et al.* (*12*). As the reduction temperature increases the OH peak becomes larger. This is also reflected in the steady increase of the FWHM observed in Table 3.

Tables 4 and 5 show a similar behavior of the Co and La peaks in both the Th- and Sr-containing oxides. However, the O1$s$ behaves quite differently in both cases. In $La_{0.8}Th_{0.2}CoO_3$ (Table 4) the O1$s$ BE increases a little but its FWHM remains small and constant. No distinguishable OH signal was detected at any reduction temperature. Table 5, on the other hand, shows that the O1$s$ BE shifts 3 eV even after reduction at 250°C. In this case, the lattice oxygen signal is lost under the tail of the OH signal. The peaks are as narrow as in the former case (Table 4) but displaced to a higher BE (532.7 ± 0.1 eV), otherwise meaning that the surface is completely covered by hydroxyls which even penetrate a few layers

TABLE 5

Binding Energies and FWHMs of $La_{0.6}Sr_{0.4}CoO_3$ Reduced in Dry $H_2$[a,b]

| Reduction temperature (°C) | Co2$p_{3/2}$ | | La3$d_{5/2}$ | | O1$s$ | |
|---|---|---|---|---|---|---|
| | BE (eV) | FWHM (eV) | BE (eV) | FWHM (eV) | BE (eV) | FWHM (eV) |
| Oxide | 781.0 | 4.7 | 834.9 | 7.1 | 529.7 | 2.2 |
| 250 | 781.1 | 5.7 | 835.2 | 7.1 | 532.8 | 2.2 |
| 300 | 779.0 | 3.3 | 835.3 | 6.7 | 532.8 | 2.2 |
| 350 | 779.1 | 2.2 | 835.4 | 6.7 | 532.7 | 2.2 |
| 400 | 779.2 | 2.2 | 835.3 | 6.5 | 532.8 | 2.3 |
| 450 | 779.2 | 2.5 | 835.4 | 6.6 | 532.6 | 2.3 |
| 500 | 779.3 | 2.1 | 835.4 | 6.5 | 532.6 | 2.6 |

[a] See footnotes in Table 3.

[b] The Sr3$d$ BE and FWHM remained constant throughout the reduction process at 134.7 ± 0.3 and 3.6 ± 0.2 eV, respectively.

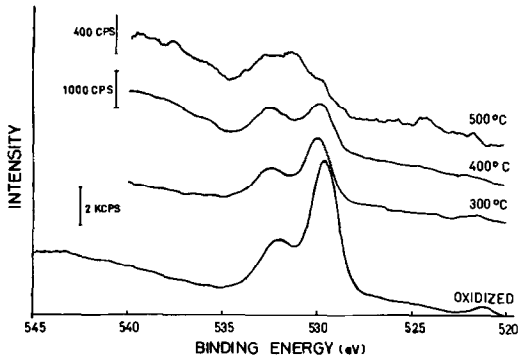


FIG. 4. O1*s* spectra of $LaCoO_3$ before and after reduction at different temperatures (see Fig. 3 legend).

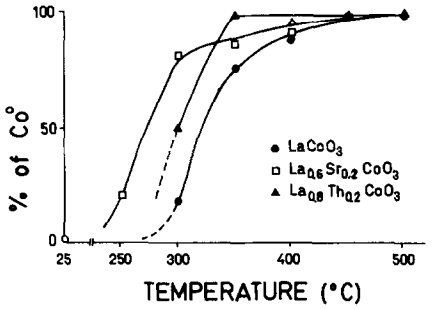


FIG. 6. Surface concentration of metallic cobalt on the reduced oxides. Values obtained from deconvolution of the Co2$p_{3/2}$ peaks. For experimental conditions see Fig. 5.

into the oxide. Neither the Sr nor the Th signals were affected by the hydrogen treatment as reported in Tables 4 and 5.

Using the XPS data the atomic fractions of La, Th, Sr, and Co were plotted vs reduction temperature for the three kinds of oxides (Fig. 5). In all cases it is seen that the surface cobalt concentration sharply increases at reduction temperatures above 300°C. Besides, in the Sr-containing oxides this element also migrated toward the surface at higher reduction temperatures.

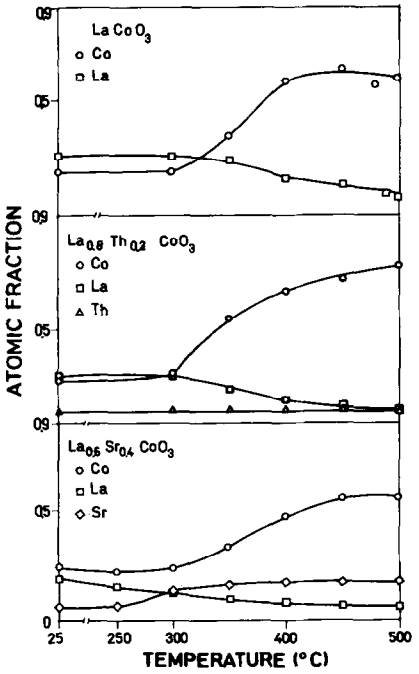


FIG. 5. Surface concentration of cations as a function of reduction temperature. $p_{H_2} \simeq 1$ atm, trap cooled at liquid air temperature.

Through deconvolution of the Co2*p* signal it was possible to calculate the percentage of $Co^0$ in the surface volume analyzed by XPS. The results obtained are shown in Fig. 6.

*Experiments run with the trap at room temperature.* The main differences noted in these experiments when compared to the former ones are (i) longer reduction times to reach equilibrium (6 vs 2 h), (ii) no surface enrichment of cobalt, and (iii) lower extents of surface reduction at each temperature. The main element on the surface after reduction is now the oxygen (or hydroxyl groups).

The XPS data for these experiments are

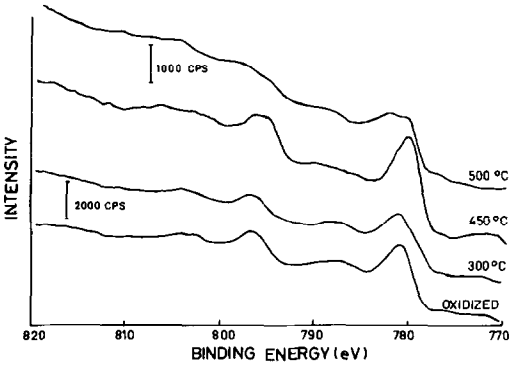


FIG. 7. Effect of the water produced during reduction upon the Co2*p* spectra of $LaCoO_3$.

TABLE 6

Binding Energies and FWHMs of $LaCoO_3$ Reduced in Wet $H_2$[a]

| Reduction temperature (°C) | Co2$p_{3/2}$ | | La3$d_{5/2}$ | | O1$s$ | |
|---|---|---|---|---|---|---|
| | BE (eV) | FWHM (eV) | BE (eV) | FWHM (eV) | BE (eV) | FWHM (eV) |
| Oxide[b] | 780.6 | 4.3 | 834.7 | 6.9 | 529.7 | 1.8 |
| 300 | 780.7 | 4.9 | 834.9 | 6.7 | 529.9 | 3.4 |
| 350 | 780.6 | 5.8 | 834.9 | 6.7 | 530.0 | 3.6 |
| 400 | 781.0 | 5.9 | 835.0 | 6.8 | 530.0 | 4.1 |
| 450 | 779.3 | 3.9 | 834.8 | 6.8 | 529.9 | 4.2 |
| 500 | 778.9 | 5.8 | 835.5 | 6.3 | 530.9 | 3.1 |

[a] The reduction was carried out in the same pretreatment chamber but the trap was left at room temperature, $p_{H_2} \simeq 1$ atm.
[b] Evacuation at 400°C.

shown in Tables 6 to 8. In Table 6 and Fig. 7 it is clearly seen that the Co2$p$ peak width goes through a minimum at 450°C in coincidence with a maximum in $Co^0$ concentration for the $LaCoO_3$. The La3$d$ doublets are very much unaffected by the treatment, except for a small displacement toward higher BE. The O1$s$ signal which is again made up by the overlapping of two peaks shows an increasing contribution of the higher BE peak as the reduction temperature goes up (Fig. 8). The shoulder at around 534 eV could indicate the presence of adsorbed water.

For the Th-substituted oxide, Table 7 shows a steady increase in cobalt reduction, narrower O1$s$ peaks compared to those observed in $LaCoO_3$ (Table 6), and no change in the Th peak after hydrogen treatment.

In the case of $La_{0.6}Sr_{0.4}CoO_3$ Table 8 shows wide Co2$p$ peaks at all reduction temperatures, a sharp increase in both BE and FWHM of the O1$s$ peak, and again no change of the Sr peak after hydrogen treatment.

Figure 9 shows the surface concentration of the elements calculated from the XPS data. At variance with the results obtained in the absence of water (Fig. 5) the cobalt

TABLE 7

Binding Energies and FWHMs of $La_{0.8}Th_{0.2}CoO_3$ Reduced in Wet $H_2$[a,b]

| Reduction temperature (°C) | Co2$p_{3/2}$ | | La3$d_{5/2}$ | | O1$s$ | |
|---|---|---|---|---|---|---|
| | BE (eV) | FWHM (eV) | BE (eV) | FWHM (eV) | BE (eV) | FWHM (eV) |
| Oxide | 781.0 | 4.3 | 834.9 | 7.0 | 530.0 | 2.0 |
| 300 | 781.2 | 4.9 | 835.2 | 7.0 | 530.1 | 2.4 |
| 350 | 781.3 | 5.8 | 835.3 | 6.9 | 530.3 | 2.5 |
| 400 | 779.4 | 5.9 | 835.3 | 7.0 | 530.3 | 2.7 |
| 450 | 779.4 | 6.4 | 835.1 | 7.1 | 530.2 | 3.0 |
| 500 | 779.0 | 4.3 | 835.2 | 7.1 | 530.0 | 3.5 |

[a] See footnotes in Table 6.
[b] The Th4$f_{7/2}$ BE and FWHM remained constant at 334.1 ± 0.1 and 2.0 ± 0.2 eV, respectively.

TABLE 8

Binding Energies and FWHMs of $La_{0.6}Sr_{0.4}CoO_3$ Reduced in Wet $H_2$[a,b]

| Reduction temperature (°C) | Co2$p_{3/2}$ | | La3$d_{5/2}$ | | O1$s$ | |
|---|---|---|---|---|---|---|
| | BE (eV) | FWHM (eV) | BE (eV) | FWHM (eV) | BE (eV) | FWHM (eV) |
| Oxide[b] | 780.9 | 4.8 | 834.8 | 6.9 | 529.8 | 2.0 |
| 300 | 781.1 | 5.1 | 834.9 | 6.8 | 532.5 | 4.5 |
| 350 | 778.9 | 4.5 | 834.8 | 6.9 | 532.3 | 5.2 |
| 400 | 781.0 | 5.4 | 834.6 | 6.7 | 532.5 | 3.6 |
| 450 | 779.4 | 5.5 | 835.3 | 7.1 | 532.5 | 4.2 |
| 500 | 779.2 | 5.5 | 835.1 | 7.1 | 532.5 | 3.9 |

[a] See footnotes in Table 6.

[b] The Sr3$d$ BE and FWHM remained constant at 134.7 ± 0.3 and 3.8 ± 0.2 eV, respectively.

concentration on the surface slightly decreases with increasing reduction temperature. On the other hand, the Th, Sr, and La atomic fractions are not affected much by this change in atmosphere.

Figure 10 shows the surface concentration of $Co^0$ and should be compared to Fig. 6. In the presence of water in no case the $Co^0$ concentration reaches 100%. Besides, in both $LaCoO_3$ and $La_{0.6}Sr_{0.4}CoO_3$ this concentration reaches a maximum at intermediate reduction temperatures. This is consistent with the data reported in Tables 6 and 8 for both the BE and FWHM of Co2$p$ at different reduction temperatures.

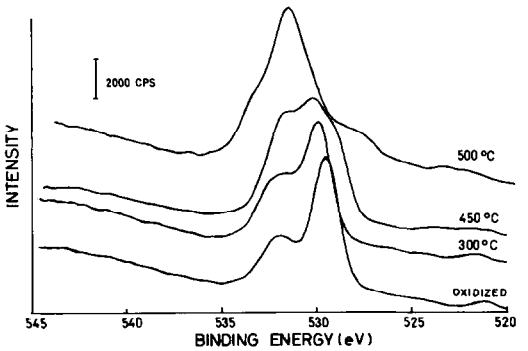


FIG. 8. Effect of the water produced during reduction upon the O1$s$ spectra of $LaCoO_3$.

DISCUSSION

The water produced during the reduction of these mixed oxides strongly affects the extent of oxygen extraction from the lattice. It has been shown that under other-

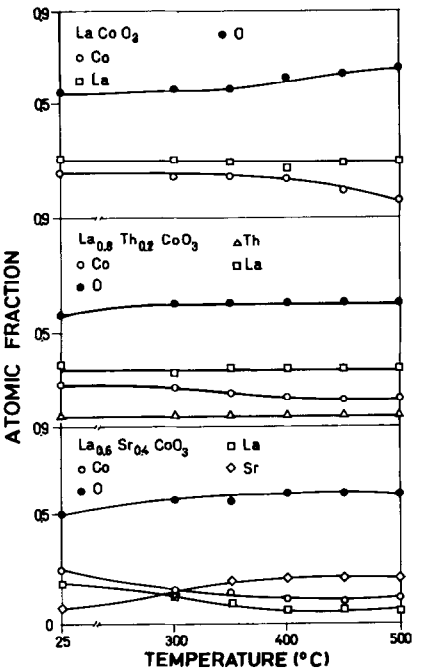


FIG. 9. Effect of the water produced along the reduction process upon the surface concentration of cations. $p_{H_2} \simeq 1$ atm.

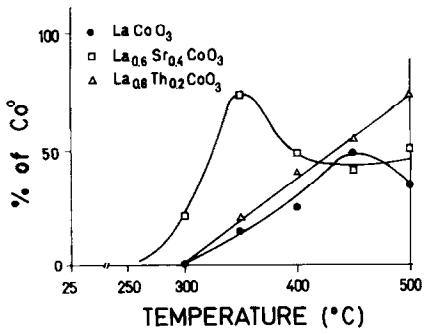


FIG. 10. Effect of the water produced during reduction upon the $Co^0$ surface concentration. $p_{H_2} \approx 1$ atm.

wise identical conditions the elimination of the water assured a faster and deeper reduction of the solid, which was always accompanied by an important segregation of cobalt to the surface.

Another general trend was observed at reduction temperatures $\geq$300°C, namely, the surface enrichment in hydroxyl groups. This effect increased in the direction Th < La < Sr, as expected from the similar trend of the Pauling electronegativity values. The hydroxyl concentration was higher in the presence of wet hydrogen. It may be that this increased hydroxyl population of the solid surface impairs the diffusion of the lattice oxygen during the reduction process.

Let us now discuss in more detail the reduction behavior of each mixed oxide.

*$LaCoO_3$*

The bulk reduction of this perovskite occurs in two steps according to Eqs. (1) and (2). The XPS data obtained in the absence of water are consistent with a similar stepwise mechanism occurring at the surface level. Upon reduction at 300°C the Co2*p* spectrum widens up and the BE shifts down 1.4 eV (Table 3) due to the coexistence of the three possible oxidation states with a rather small contribution of $Co^0$ (Fig. 6). The Co/La ratio is not altered by this mild reduction (Fig. 5). Between 300 and 350°C the Co2*p* peaks are drastically reduced in width and the Co/La ratio increases. These results seem to indicate that the onset of the second reaction (Eq. (2)) at the surface level occurs in this temperature range.

In the presence of water vapor it seems that the second reaction is impaired. The XPS spectra shows that metallic cobalt appears at higher temperatures and much lower concentrations (Table 6 and Fig. 10). Furthermore, this surface concentration shows a maximum at 450°C. This effect has been observed before by Lombardo *et al.* (*6*) who used a VG ESCA 3 instrument which has a larger pretreatment chamber (~10 liters) attached. In their experiments the reduction was carried out without a cold trap. Their results were between those reported here with and without the cold trap. This is consistent with the fact that the partial pressure in the VG pretreatment chamber was about one order of magnitude lower than in the experiments reported here when the trap was left at room temperature.

Lombardo *et al.* (*6*) did not find a cobalt enrichment of the surface but this element was completely reduced to its metallic state and then reoxidized at higher reduction temperatures. Besides, by rotating the sample holder and in so doing modifying the ejection angle of the electrons, they were able to ascertain that this reoxidation process scarcely affected more than one surface layer.

The observation made here about the marked increase of the higher BE peak contributing to the O1*s* spectrum as the reduction temperature is raised (Tables 3 and 6) may lend an explanation to this reoxidation process which apparently occurs in the presence of hydrogen at high temperatures ($\geq$400°C), but in reality proceeds during evacuation. When the hydrogen is removed and the surface hydroxyl concentration is high enough, the cobalt may be reoxidized and probably covered with a monolayer of oxide.

This redox process is known to occur in other catalyst systems such as $Mo(CO)_6/\gamma$-$Al_2O_3$ (*13*). Upon evacuation at temperatures as low as 200°C the $Mo^V$ EPR signal

develops and $H_2$ is detected in the gas phase. In our case, the temperature required for the reoxidation of cobalt is strongly dependent on the OH surface concentration.

The XPS spectra recorded after reduction in the absence of water vapor do not show the reoxidation of the cobalt. This may be due to the massive segregation of cobalt that occurs in this case which could make difficult to detect a single layer of oxidized cobalt in the Co2*p* spectrum. An indirect proof of the formation of this oxide layer may be obtained from Fig. 11a which shows a steady increase of the Co/La ratio while the Co/O ratio goes through a maximum at 400–450°C reduction temperature. Since at this point only $Co^0$ is seen by XPS the Co/O curve should follow the Co/La one. The maximum may then be an indication that the O1*s* spectrum shows a composite of oxygen peaks coming not only from $La_2O_3$ or $La(OH)_3$ but also from the top of the cobalt clusters as well. In fact, assuming that only $La(OH)_3$ and $Co^0$ are present after reduction at 500°C, the Co/O ratio should be three times smaller than the Co/La ratio. Figure 11a shows this factor to be about 5, meaning that there is a large excess of oxygen in the surface, which is very likely bound to the top of the cobalt clusters.

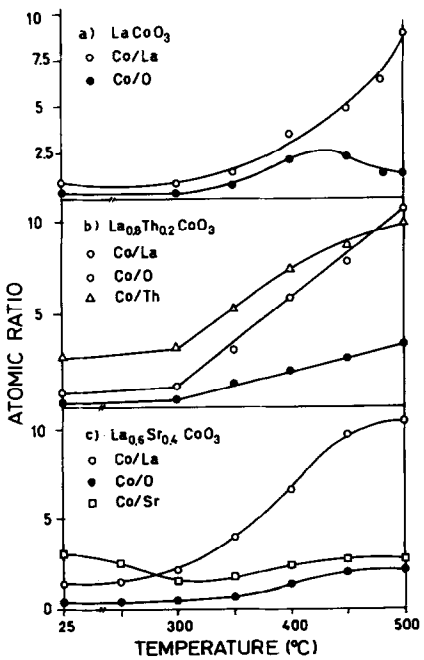


FIG. 11. Effect of reduction temperature upon the XPS calculated atomic ratios of the elements. Trap with liquid air, $p_{H_2} \simeq 1$ atm.

### $La_{0.8}Th_{0.2}CoO_3$

The presence of Th reduces to a minimum the formation of hydroxyls, even in the presence of water vapor (Tables 4 and 7). As a consequence of this the $Co^0$ is not reoxidized at high reduction temperatures (Figs. 6 and 10). It may be that the higher acidity of thorium reduces the ability of lanthanum to form the hydroxide on the surface.

Comparing Figs. 11a and 11b the different behavior of the Co/O ratio in the two oxides is noted. In the Th-substituted solid the absence of a maximum in this ratio would also indicate that no reoxidation of the cobalt occurs.

The above results are then consistent with a model in which clusters of $Co^0$ are formed on the surface of the oxide which apparently increase in size at temperatures above 350°C. These clusters are not reoxidized upon evacuation, as was the case in $LaCoO_3$, due to the scarcity of hydroxyls on the surface of the reduced oxide.

### $La_{0.6}Sr_{0.4}CoO_3$

The main differences in the behavior of this oxide when compared to the previous ones may be caused by the migration of SrO toward the surface which begins at or around 250°C (Figs. 5 and 8). This is likely to be connected with the high concentration of hydroxyls seen on this sample, which almost completely blocks the lattice oxygen peak at reduction temperatures higher than 350°C (Table 5).

Since the cobalt starts to migrate at higher temperatures than the Sr, the Co/Sr ratio reaches a minimum around 300°C (Fig. 11c). However, due to the facile re-

duction of this mixed oxide (Table 2), the $Co^0$ concentration at 300°C is significantly higher in this case than in the other two oxides (Figs. 6 and 10). It is then expected that this solid will show a peculiar catalytic behavior greatly influenced by the severity of the hydrogen pretreatment; e.g., the presence of the segregated SrO or $Sr(OH)_2$ could modify the selectivity in a given reaction system as shown elsewhere (*14*).

*Reduction Model*

The model proposed earlier for the reduction of $LaCoO_3$ (*6*) can be improved and extended to other related oxides.

The bulk and surface reduction data obtained at each temperature have been plotted in Fig. 12. The surface values were calculated assuming that in those cases in which the $Co^0$ peak contribution was higher than 25% the remaining cobalt was present as $Co^{2+}$. This assumption was made because it is very difficult to ascertain by deconvolution the proportion of $Co^{2+}$ and $Co^{3+}$ due to the close vicinity of these wide peaks. The assumption is based upon the detection through XRD of the intermediate compound $La_4Co_3O_{10}$ along the reduction process (*15, 16*). This compound which is equivalent to $LaCo_{0.75}O_{2.5}$ in Eq. (1), is further reduced to $La_2Co^{II}O_4$ and/or $Co^0/La_2O_3$.

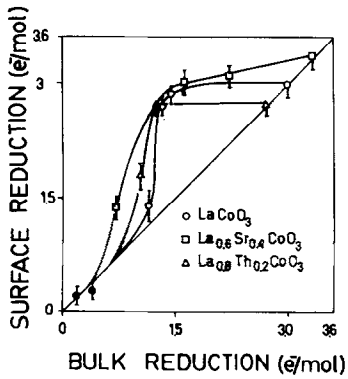


FIG. 12. Correlation between surface reduction, determined by XPS, And bulk reduction, calculated from the hydrogen uptake in a gas recirculating system. (●) from Ref. (*6*).

Figure 12 shows that at low extents of reduction the solid is homogeneously reduced. At around 1.5 electrons/molecule (bulk) the maximum difference between bulk and surface oxidation states occurs. This means that a change in reduction regime has occurred; the process has become diffusion limited. Beyond this point the surface layer seen by XPS (20–30 Å deep) is almost fully reduced, but the temperature must be increased up to 500°C to completely reduce the bulk.

The change in regime occurs between 300 and 350°C for both $LaCoO_3$ and the Th-containing cobaltate. In the Sr-substituted oxide this transition interval moves down 50°C. In fact, within this temperature ranges is when the cations start to migrate as shown in Fig. 5.

It is interesting to note that in these mixed oxides, despite the early appearance of metallic centers that could activate the hydrogen, the reduction rate is not accelerated as in the case of Group VIII oxides, e.g., NiO (*17, 18*) and cobalt oxides (*18*). This may be due to the formation of estable oxides containing the transition metal in a lower oxidation state. As mentioned above, the existence of other very estable oxides has been documented in the case of the lanthanum–cobalt–oxygen system (*15*).

An interesting question arises from the catalytic standpoint: What happens with the cobalt exposed on the surface as the reduction temperature increases?

A schematic model is shown in Fig. 13. The most stable system is no doubt the Th-substituted oxide. This oxide does not show a tendency to adsorb water, the hydroxyl surface concentration is low, and therefore the cobalt clusters are not easily reoxidized.

$LaCoO_3$ and $La_{0.6}Sr_{0.4}CoO_3$ show enhanced affinity to react with the reduction water when treated in hydrogen at increasing temperatures. The high concentration of surface hydroxyls increases the driving force to reoxidize the cobalt clusters. In fact, it has been shown that due to this ox-

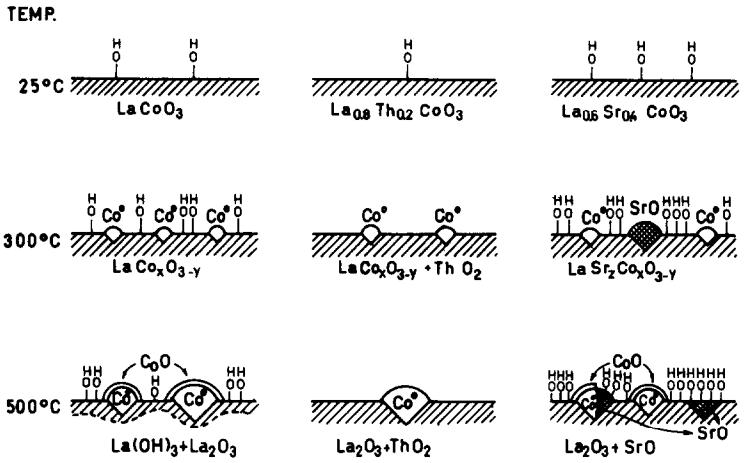


FIG. 13. Reduction model of the three mixed oxides.

ide layer both the catalytic activity and the CO chemisorption ability (*1*) are strongly affected at low temperatures (−20°C). However, this is not the case when a strongly reducing reacting mixture is contacted with the prereduced oxide at elevated reaction temperatures. The catalytic results and the titration data reported in the following paper (*14*) are consistent with this model. Particularly, they suggest that SrO and $Co^0$ are in contact after reduction at high temperature. This could not be verified, however, through the spectroscopic studies reported here.

ACKNOWLEDGMENTS

We are indebted to the Japan International Cooperation Agency for the donation of an ESCA 750 Shimadzu spectrometer. This work was supported by grants from CONICET and SECyT.

REFERENCES

1. Petunchi, J. O., Ulla, M. A., Marcos, J. A., and Lombardo, E. A., *J. Catal.* **70,** 356 (1981).
2. Ulla, M. A., Miró, E. A., and Lombardo, E. A., *Actas VIII Simp. Iberoamer. Catal. B* **20,** 475.
3. Nudel, J. N., Umansky, B. S., Piagentini, R. O., and Lombardo, E. A., *J. Catal.* **89,** 362 (1984).
4. Sis, L. B., Wirtz, G. P., and Sorenson, S. C., *J. Appl. Phys.* **44,** 5553 (1973).
5. Crespin, M., and Hall, W. K., *J. Catal.* **69,** 359 (1981).
6. Lombardo, E. A., Tanaka, K., and Toyoshima, I., *J. Catal.* **80,** 340 (1983).
7. Voorhoeve, P. J. H., *in* "Advanced Materials in Catalysis" (J. J. Burton and R. L. Garten, Eds.), p. 129. Academic Press, Orlando, FL, 1977.
8. Miró, E., Flesia, M., and Lombardo, E. A., *Rev. Fac. Ing. Quim* **44,** 15 (1980).
9. Johnson, D. W., and Gallagher, P. K., *in* "Ceramic Processing before Firing" (G. Onoda, Jr., and L. Hench, Eds.), p. 125. Wiley, New York, 1978.
10. Gallagher, P. K., Johnson, D. W., Jr., and Vogel, E. M., *J. Amer. Cer. Soc.* **60,** 28 (1977).
11. Wagner, C. D., Riggs, W. M., Davis, L. E., Moulder, J. F., and Muilenberg, G. E., (Eds.), *in* "Handbook of X-ray Photoelectron Spectroscopy." Perkin–Elmer Corp. Palo Alto, CA, 1978.
12. Fleisch, T. H., Hicks, R. F., and Bell, A. T., *J. Catal.* **87,** 398 (1984).
13. Brenner, A., and Burwell, L., Jr., *J. Catal.* **52,** 353 (1978).
14. Ulla, M. A., Migone, R. A., Petunchi, J. O., and Lombardo, E. A., *J. Catal.* **105,** 107–119 (1987).
15. Seppanen, M., Kytö, M., and Taskinen, P., *Scand. J. Metall.* **9**(3), 255 (1980).
16. Marcos, J., Ph.D. thesis, Universidad del Litoral, Santa Fe, (1986).
17. Hurst, N. W., Gentry, S. J., Jones, A., and McNicol, B. D., *Catal. Rev. Sci. Eng.* **24**(2), 233 (1982).
18. Delmon, B., *in* "Introduction a la Cinétique Hétérogéne," p. 255. Technip, 1969.